Polymer Degradation and Stability 133 (2016) 162–173

Contents lists available at ScienceDirect

Polymer Degradation and Stability

journal homepage: www.elsevier.com/locate/polydegstab

Synthesis of a novel bridged-cyclotriphosphazene flame retardant and its application in epoxy resin

Bin Zhao [a], Wen-Jun Liang [a], Jun-Sheng Wang [b], Fei Li [a], Ya-Qing Liu [a, *]

[a] Research Center for Engineering Technology of Polymeric Composites of Shanxi Province, North University of China, Taiyuan 030051, China
[b] Tianjin Fire Research Institute of the Ministry of Public Security, Tianjin 300381, China

ARTICLE INFO

Article history:
Received 1 May 2016
Received in revised form
10 August 2016
Accepted 23 August 2016
Available online 25 August 2016

Keywords:
Flame-retardant
Epoxy resin
Phosphazene
Thermal degradation
Cone calorimeter

ABSTRACT

A novel flame retardant, named bisphenol-A bridged penta(anilino)cyclotriphosphazene (BPA-BPP), was successfully synthesized. Its chemical structure was characterized by Fourier transform infrared (FTIR), ^{1}H NMR and ^{31}P NMR. Then, different amounts of BPA-BPP were mixed with diglycidyl ether of bisphenol-A (DGEBA) to fabricate flame retardant epoxy resin (EP). Nonisothermal differential scanning calorimetry (DSC) and thermogravimetric analysis (TGA) tests were used to study the curing kinetics and thermal degradation behaviors of flame retardant EPs. The results of limiting oxygen index (LOI), vertical burning tests (UL-94) suggested that BPA-BPP exhibited good flame-retarded efficiency on the EP loaded with low phosphorus content. Compared with the neat EP, the LOI value of EP/9%BPA-BPP increased from 21.0 vol% to 28.7 vol%. Furthermore, the peak of heat release rate (PHRR), total heat release (THR), total smoke production (TSP) of the same sample, obtained from cone calorimetry, were declined obviously, suggesting excellent flame retardancy and smoke inhibition. The morphology and chemical structures of the char layers were analyzed by SEM, Raman and FTIR. The Py-GC/MS was used to investigate the pyrolysis behavior and flame-retardant mechanism of BPA-BPP. In the process of heating, aniline, diphenylamine and NH_3 were released from BPA-BPP in gaseous phase, and phosphorus-rich carbonaceous chars were left in condensed phase. BPA-BPP could promote EP to form intumencent protective char layers, enhancing flame retardancy of EP effectively.

1. Introduction

Epoxy resins (EPs) have been widely applied as matrix resin in many fields due to their ease of curing and processing, good dimensional stability, superior electrical, chemical and mechanical properties [1–3]. However, inflammability of epoxy resin limits their wide-spread application in fields requiring high fire resistance. Although traditional halogen-containing EPs have been well developed to meet the considerable secure requirements in these fields, halogen additives will cause environmental toxicity as well as health hazards because of the generation of highly toxic and potentially carcinogenic substances during combustion [4,5]. Therefore, a growing interest has been focused on halogen-free solutions, which allows for green chemistry and sustainable development [6,7].

Over the past decade, many efforts have been made to achieve high flame retardancy of EPs by using phosphorus- and nitrogen-containing additives [8–10], monomers [5,11] or hardeners [12,13]. Among them, phosphazene derivatives have aroused great attention due to they are good candidates as the flame retardants for EPs [10,11,14,15]. On one hand, cyclotriphosphazene as the matrix of phosphazene derivatives can provide the synergism of the phosphorus-nitrogen combination, which result in good fire resistance and auto-extinguish ability in polymers [16–19]. This advantage could be ascribed to its unique molecular framework of cyclotriphosphazene based on alternation of P and N atoms in a conjugative mode [20]. On the other hand, substitution chemistry at phosphorus atoms particularly provides a multiple synthetic methodology for creating cyclotriphosphazene-based derivatives with varied substituent groups, which allows us to obtain multifunctional reactive and additive types flame retardants with ease [21–23]. Researchers have paid much attention to obtain new derivatives of cyclotriphosphazene to prepare flame retardant EPs [11,14,15,24]. These studies display clearly that the cyclotriphosphazene structure contribute to high char-yield and excellent self-extinguish ability in EPs.

* Corresponding author.
E-mail address: lyq@nuc.edu.cn (Y.-Q. Liu).

http://dx.doi.org/10.1016/j.polymdegradstab.2016.08.013
0141-3910/

In this work, a novel flame retardant bisphenol-A bridged penta (anilino) cyclotriphosphazene (BPA-BPP) was synthesized successfully through nucleophilic substitution reaction of hexachlorocyclotriphosphazene, bisphenol-A and aniline. The chemical structure of BPA-BPP was characterized via Fourier transform infrared spectroscopy (FT-IR), ^{1}H NMR, and ^{31}P NMR. Then flame-retardant EPs with 3 wt%, 6 wt% and 9 wt% BPA-BPP were prepared and studied. The results of the thermogravimetric analysis (TGA), LOI, UL-94, microscale combustion calorimeter (MCC) and cone calorimeter revealed that the incorporation of BPA-BPP changed the thermal degradation behavior and enhanced the flame retadancy of EP. Meanwhile, the graphitizing structure and morphology analysis of the residual chars as well as pyrolysis behavior of BPA-BPP have been investigated systematically.

2. Experimental

2.1. Materials

Hexachlorocyclotriphosphazene (HCCP) was obtained from Zibo Lanyin Chemical Co., Ltd., (Zibo, China), purified by recrystallization from *n*-heptane prior to use. Bisphenol-A (BPA), aniline and 4,4′-Diamino-diphenylmethane (DDM) were purchased from Aladdin Industrial Corporation, (Shanghai, China). Potassium carbonate (K_2CO_3), Sodium hydride (NaH), sodium sulfate (Na_2SO_4), potassium hydroxide (KOH), tetrahydrofuran (THF), petroleum ether, dichloromethane (CH_2Cl_2), ethyl ether and *n*-heptane were purchased from Tianjin Guangfu Fine Chemical Research Institute, (Tianjin, China). THF was distilled from sodium benzophenone ketal before use, and the other chemicals and reagents were used without further purification. Diglycidyl ether of bisphenol-A (DGEBA) (NPEL128, epoxide equivalent weights = 185 g/equiv) was commercially available.

2.2. Synthesis of bisphenol A bridged chlorocyclotriphosphazene (BPA-BCP)

NaH (60% in mineral oil, 4.0 g) was added to a solution of HCCP (34.8 g) in THF at −20 °C under nitrogen protection. A solution of BPA (11.4 g) in THF was added dropwise into the suspension over 2 h with agitation, followed by stirring for 12 h at −20 °C. Then solution was stirred for 2 h at room temperature. After the reaction was completed, the reaction mixture was filtered and then washed repeatedly with deionized water. The organic layer was dried with anhydrous Na_2SO_4 and concentrated on a rotator evaporator under reduced pressure, leaving a white solid. The residue was purified by silica gel chromatography (silica gel, 40 vol% of CH_2Cl_2/60 vol% of petroleum ether) to obtain white solid of BPA-BCP (31.9 g, yield 75.1%). M.p.: 114.0–114.9 °C; ^{1}H NMR (DMSO-d_6, TMS): δ/ppm 7.19–7.17 (d, 4H), 7.09–7.07 (d, 4H), 1.62 (s, 6H); ^{31}P NMR (DMSO-d_6, 85% H_3PO_4): δ/ppm 22.74–22.35 (d, 2P) and 12.12–11.35 (t, 1P); FTIR: ν/cm^{-1} = 1180 and 1150 (P═N), 1014 and 967 (P–*O*–C), 591 and 515 (P–Cl).

2.3. Synthesis of bisphenol A bridged penta(anilino) cyclotriphosphazene (BPA-BPP)

BPA-BCP (25.5 g) was added to a suspension of K_2CO_3 (41.5 g) in aniline (93.1 g) under nitrogen protection. This reaction mixture was stirred at room temperature for 2 h. Then it was heated to 150 °C and maintained for 8 h. Subsequently, the mixture was cooled to room temperature prior to filtration. The excess aniline was removed under reduced pressure yielding brown solid. The solid was treated with aqueous KOH and extracted with diethyl ether. Finally, the diethyl ether solution was added into petroleum ether (200 mL), then the white precipitate formed and the solvent was removed by filtration. The precipitate was washed with petroleum ether (100 mL) and dried under vacuum for 12 h. The white product BPA-BPP was obtained in 87.3% yield (37.1 g). M.p.: 109.0–110.4 °C; ^{1}H NMR (DMSO-d_6, TMS): δ/ppm 7.41 (s, 4H), 7.29 (s, 4H), 7.24–7.11 (m, 20H), 7.06–6.99 (m, 30H), 6.73–6.66 (m, 10H), 1.37 (s, 6H); ^{31}P NMR (DMSO-d_6, 85% H_3PO_4): δ/ppm 8.88–8.19 (t, 1P) and 2.85–2.51 (d, 2P); FTIR: ν/cm^{-1} = 3361 (–NH–), 1173 and 1150 (P═N), 1029 and 1000 (P–*O*–C).

2.4. Preparation of epoxy thermosets

EP/BPA-BPP samples were prepared via a thermal curing process. At first, BPA-BPP and DDM were mixed at 120 °C for 20 min, giving a homogenous liquid. DGEBA was previously heated to 50 °C. The mixture of BPA-BPP and DDM was added into DGEBA under vigorous stirring. It was degassed under vacuum for 10 min to remove trapped air, then poured directly into a preheated teflon mould. A two-step curing procedure was carried out to obtain the thermosetting resins. The epoxy mixture was cured in air convection oven for 2 h at 90 °C and then 2 h at 130 °C. All the details of formula are listed in Table 1.

2.5. Measurement and characterization

Fourier transform infrared (FTIR) spectra were directly recorded by attenuated total reflection (ATR) adjunct of Nicolet IS50 spectrometer over the frequency range from 500 to 4000 cm^{-1}, the resolution factor of FTIR spectrometer was 4 cm^{-1} and 16 scans.

^{1}H NMR and ^{31}P NMR spectra were conducted on a Bruker AV II-400 MHz at room temperature using DMSO-d_6 as the solvent.

The curing kinetics of EP/DDM and EP/DDM/BPA-BPP samples were studied by nonisothermal differential scanning calorimetry (DSC) testing (DSC-1, METTLER TOLEDO), operating at a heating rate of 5, 10, 15 and 20 °C/min under nitrogen atmosphere.

Thermogravimetric analysis (TGA) was performed on a TA Instruments Q50 thermal gravimetric analyzer in a temperature range of 40–700 °C at a heating rate of 10 °C/min, and sample weight was in the range of 6–8 mg. According to our TGA measurement, the residue mass reproduction of each sample was within ±1%.

Limiting oxygen index (LOI) test was accorded to standard method ASTM D2863-00 performing with a Motis oxygen index test instrument (Suzhou, China). The dimensions of the specimen were 130 mm × 6.5 mm × 3.2 mm. The Vertical burning tests (UL-94) were measured on CZF-5 instrument (Nanjing Jiangning Instrument Factory, China) based on ASTM D3801/UL-94V standard. The sample size was 125 mm × 13 mm × 3.2 mm.

Pyrolysis combustion flow calorimeter (PCFC) tests were performed using a FAA Microscale combustion calorimeter (Fire Testing Technology, UK) according to ASTM D7390. 5 ± 0.5 samples were heated from 100 to 700 °C at a heating rate of 1 °C/s at a nitrogen flowing rate of 80 mL/min. The fire behavior of the EPs was evaluated via a cone calorimeter device (Fire Testing Technology,

Table 1
Formulas of the cured EP composites.

Sample	DGEBA (g)	DDM (g)	BPA-BPP	
			(g)	(wt%)
EP	80	21.5	–	–
EP/3%BPA-BPP	80	21.5	3.1	3.0
EP/6%BPA-BPP	80	21.5	6.5	6.0
EP/9%BPA-BPP	80	21.5	10.0	9.0

East Grinstead, UK) according to ISO 5660-1. The foursquare samples with the dimension of 100 × 100 × 3 mm^3 were exposed to a radiant cone at a heat flux of 35 kW/m^2. In both Micro-combustion calorimetry and Cone calorimetry tests, the data we obtained from the two parallel tests are nearly to each other (±5%), the data we reported was one of them.

Py-GC/MS analysis was conducted on a Perkin-Elmer Clarus 680 GC-SQ8MS gas chromatography-mass spectrometer equipped with a CDS 5200 pyrolyzer. The helium (He) was utilized as carrier gas for the volatile products. The injector temperature was 250 °C, 3 min at 40 °C then the temperature was increased to 280 °C at a rate of 10 °C/min. The temperature of GC/MS interface was 280 °C and the cracker temperature was 500 °C.

Scanning electron microscopy (SEM) was performed on a JEOL JSM-6510 instrument at an acceleration voltage of 30 kV. Laser Raman spectroscopy (LRS) measurements were carried out at room temperature with a Renishaw inVia Raman spectrometer (Renishaw Co., UK) by 532 nm laser line.

The phosphorus (P) contents of BPA-BPP and the residue were determined by Inductively Coupled Plasma Optical Emission Spectrometer (ICP-OES, Thermo 7400, USA). The nitrogen (N) contents of BPA-BPP and the residue were measured by Kjeldahl method on a KDY-9820 instrument (Beijing Ruibangxingye Technologies Co., Ltd).

3. Results and discussions

3.1. Synthesis and characterization

The compound BPA-BPP was synthesized by two-step substitution reactions (Scheme 1). The precursor BPA-BCP was first synthesized by a geminal substitution reaction of BPA with a commercial product HCCP. The molecular structure of BPA-BCP was characterized by ^{1}H NMR, and ^{31}P NMR spectroscopy and FTIR spectroscopy. The ^{1}H spectrum of BPA-BCP (Fig. 1 B) shows chemical shifts of eight aromatic protons at 7.19–7.07 ppm (H_b, H_c) and six methylic protons at 1.62 ppm (H_a). As shown in Fig. 2, there are two sets of multiple resonance signals in the ^{31}P NMR spectrum of BPP-BCP. The different chemical environments for phosphorus centers of BPA-BCP result in a doublet signal at 22.74–22.73 ppm (Fig. 2 B, P_b, Cl–P^*-Cl) and a triplet one at 12.12–11.35 ppm (Fig. 2 B, P_a, C_6H_5O–P^*-Cl), which are assigned to the two phosphorus atoms bearing four chloride atoms and the mono-substituted phosphorus atom, respectively. These two different environmental phosphorus atoms of P_b and P_a give an integration ratio of 2:1. Fig. 3 shows the FTIR spectrum of BPA-BCP, which clearly displays the appearance of absorption peak at 967 cm^{-1}, representing the formation of P–*O*–C bond due to the substitution reaction between HCCP and BPA. Meanwhile, a strong P=N stretching vibration in the infrared spectrum at 1180-1150 cm^{-1} confirms the presence of phosphazene ring. The characteristic absorption peaks ascribed to the aromatic C–H of phenoxy groups are observed at 2965, 1497, 869 and 837 cm^{-1}. These characterization data indicate that the precursor BPA-BCP has been successfully synthesized.

In order to get the target product BPA-BPP, the precursor BPA-BCP was employed to react with aniline to complete the full substitution of chloride atoms in its phosphazene ring. The chemical structure of BPA-BPP was also characterized by ^{1}H NMR, and ^{31}P NMR spectroscopy and FTIR spectroscopy. Fig. 1 (A) shows the ^{1}H NMR spectrum of BPA-BPP with several sets of resonance signals. The resonance signals corresponding to the aromatic protons in the range of 7.41–7.29 ppm are typical regions for the benzene rings of the BPA- backbone (H_b, H_c). A strong singlet resonance signal at 1.37 ppm is the characteristic peak of the protons of methyl groups (H_a). Two sets of multiple resonance signals at around 7.24–6.99 ppm are corresponding to the protons of the benzene rings (H_e, H_f) and a set of multiple resonance signals at around 6.73–6.66 ppm are ascribed to the protons of the –NH (H_d). ^{31}P NMR spectrum of BPA-BPP in Fig. 2 (A) presents a set of complicated multiple resonance signals. A doublet signal at 2.85–2.51 ppm [P_b, P^*-$(NHC_6H_5)_2$] and a triplet one at 8.88–8.19 ppm [P_a, P^*-$(OC_6H_4)(NHC_6H_5)$] are attributed to the two different environmental phosphorus atoms of cyclotriphosphazene, respectively. As shown in FTIR spectrum of BPA-BPP (Fig. 3), the appearance of absorption peak at 3369 cm^{-1} represents –NH– bond formed from the substitution reaction between the remaining chlorine of the

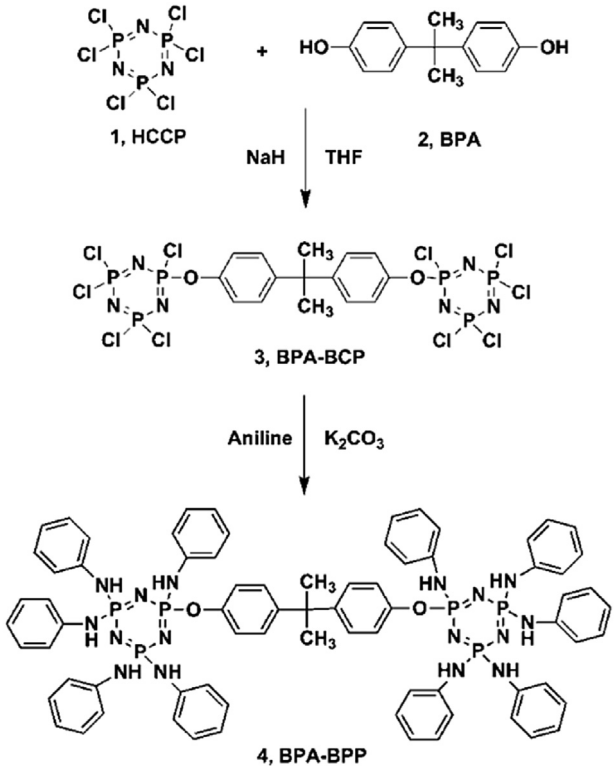

Scheme 1. Synthetic route of BPA-BPP.

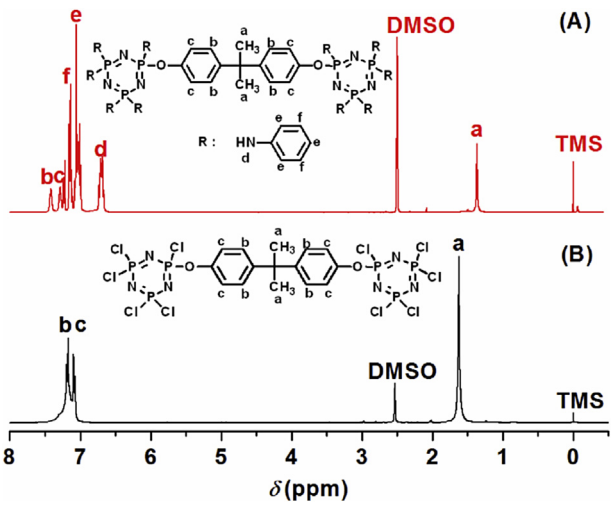

Fig. 1. ^{1}H NMR spectra of BPA-BPP (A) and BPA-BCP (B) in DMSO-d_6.

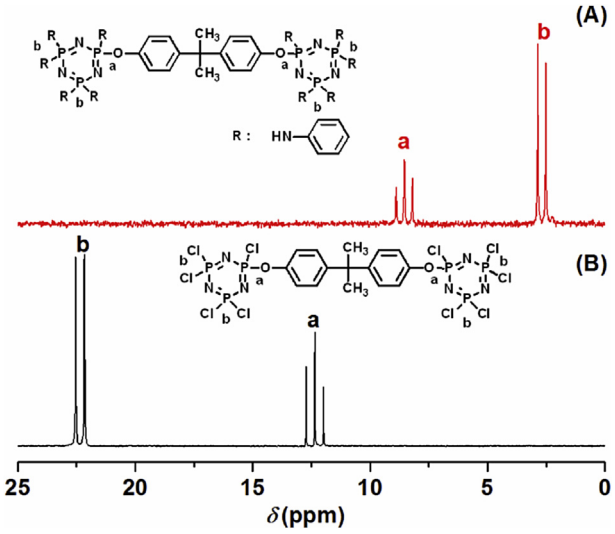

Fig. 2. ^{31}P NMR spectra of BPA-BPP (A) and BPA-BCP (B) in DMSO-d_6.

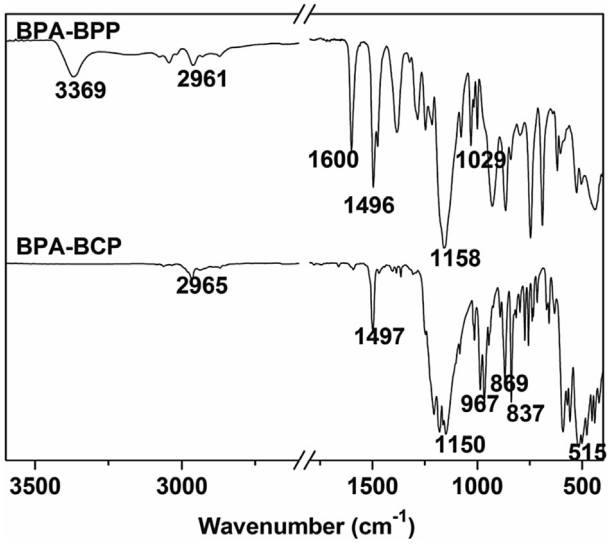

Fig. 3. FTIR spectra of BPA-BCP and BPA-BPP.

precursor BPA-BCP and aniline. An intensive absorption peaks can be observed at 1158 cm^{-1} due to the asymmetrical N–P═N stretching, indicating the presence of the phosphazene rings. In conclusion, BPA-BPP has been synthesized successfully. Furthermore, the actual phosphorus and nitrogen contents in BPA-BPP were determined by ICP-OES and Kjeldahl method, respectively. The results are shown as follows: P content, 13.8 wt % (calcd 13.1 wt %); N content, 16.9 wt% (calcd 15.8 wt%).

3.2. Thermal analysis

Can BPA-BPP react with epoxy as cured agent since there are amine groups in it? To answer this question, the curing kinetics of EP/DDM and EP/DDM/BPA-BPP (9 wt%) samples have been studied by nonisothermal DSC testing. The relevant curves and data are depicted in Fig. 4 and Table S1 (supporting information). The reaction activation energy (E_α), reaction order (n), and pre-exponential factor (A) have been calculated by the Kissinger equation combined with the Crane equation shown in Table 2. The Flynn-Wall-Ozawa equation has been also applied to verify the E_α values. The three methods are applied to calculate the kinetic parameters without any assumption about a conversion-dependent equation [12]. The curing reactions of EP as well as EP/9%BPA-BPP are both consistent with the n-order kinetic model, where the n values are equal to 0.88 and 0.87, respectively. The n value of EP/9% BPA-BPP is a little lower, suggesting its higher curing rate. Considering the E_α, the value of EP/9%BPA-BPP is lower. These results indicate that BPA-BPP can react with epoxy. However, we must declare that the curing agent (such as DDM in this system) cannot be replaced by BPA-BPP in our experiment.

Thermogravimetry analysis (TGA) of the BPA-BPP, neat EP, and EP/BPA-BPP provides additional information about their thermal stabilities and thermal degradation behaviors. Fig. 5 shows the TG and DTG curves of specimens evaluated under nitrogen and air. The relevant data are presented in Table 3. T_{onset} and T_{max} are defined as the temperature at 5% weight loss and the temperature of maximum weight loss rate, respectively; α_{max} is the maximum weight loss rate.

As shown in Fig. 5 (A, C) and Table 3, BPA-BPP displays gentle decomposition stages in both N_2 and air atmosphere. The residual char of BPA-BPP at 700 °C is as high as 58.9 wt% in N_2 and 56.1 wt% in air. This can be attributed to the high thermal stability of the phosphazene ring [25]. The TG curve of neat EP shows two degradation stages under air and single degradation stage in N_2, which are consistent with the results previously reported [26,27]. The first stage (around 400 °C) mainly involves dehydration of the material and formation of polyaromatic structures [28]. The EP/BPA-BPP reveals similar thermal degradation process with neat EP in N_2 and air. However, in both atmospheres, the T_{onset} and T_{max} of the EP/BPA-BPP composites shift to low temperature area compared with those of neat EP. These results can be explained by the degraded products of BPA-BPP catalyzed the decomposition of EP matrix. Furthermore, the T_{max} and α_{max} of EP/BPA-BPP composites are lowered with increase of flame retardant in N_2. Unlike the case in N_2, α_{max1} increase and α_{max2} decrease with the increasing contents of BPA-BPP under air atmosphere. It suggests that more flame retardants promote the decomposition of EP in low temperature whereas restrain the decomposition of EP in high temperature zone. Under both atmospheres, the residual char obtained from the EP/BPA-BPP at high temperatures (beyond 500 °C in N_2 and beyond 650 °C in air) are much higher than that from neat EP. Meanwhile, the test values of residue chars at 700 °C are higher than the corresponding calculated values. These results suggest that BPA-BPP or its pyrolytic products can react with EP matrix during heating, which effectively promote the char-forming process at lower temperatures and enhance the thermal stability of EP at higher temperatures.

3.3. Flame retardancy and fire behavior

The flame retardancy of epoxy resins with BPA-BPP was evaluated by limiting oxygen indexes (LOI) and vertical burning tests (UL-94). The relevant data are summarized in Table 4. The photographs of the EPs during UL-94 tests are shown in Fig. 6.

The LOI value of neat EP is only 21.0 vol%, which cannot extinguish spontaneously within 50 s while accompanied with flame drippings. Fig. 6 shows that neat EP are burnt out during combustion and cannot pass UL-94 test. The LOI values of EP/BPA-BPP composites increase from 21.0 to 28.7 vol% with the increasing content of BPA-BPP from 0 to 9 wt% in EP. The EP/9%BPA-BPP sample pass the UL-94 V-1 rating when the contents of BPA-BPP and phosphorus are increased to 9 wt% and 1.18 wt%, respectively. In Fig. 6, it is worth noting that the EPs containing BPA-BPP are almost no damage after UL-94 tests even though the EP/3%BPA-

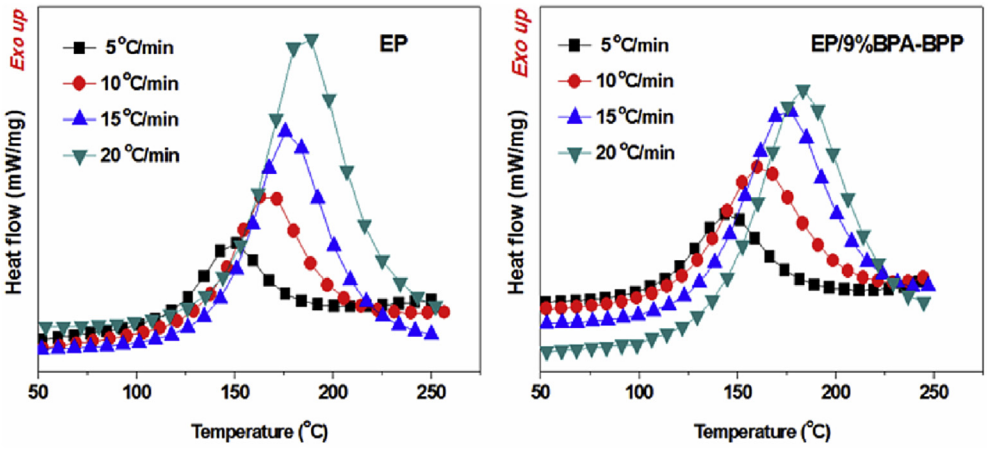

Fig. 4. DSC curves of EP and EP/9%BPA-BPP at different heating rates (Both EP and EP/9%BPA-BPP samples contained DDM as curing agent, the detailed formulas are listed in Table 1).

Table 2
Kinetic parameters of the curing reaction with or without BPA-BPP.

		EP	EP/9%BPA-BPP
Kissinger[d] and Crane eq[e]	E_α[a]	53.1	50.9
	ln A[b]	9.3	8.8
	n[c]	0.88	0.87
Flynn–Wall–Ozawa eq[f]	E_α[a]	57.4	55.3

[a] The reaction activation energy in kJ/mol.
[b] Pre-exponential factor.
[c] Reaction order.
[d] Kissinger equation: $\ln(\beta/T_p^2) = \ln\{(AR)/E_\alpha)\} - (E_\alpha/R) \times (1/T_p)$.
[e] Crane equation: $\ln \beta = -(E_\alpha/nR) \times (1/T_p) + C$.
[f] Ozawa equation: $\ln \beta + 1.0516 \times (E_\alpha/R) \times (1/T_p) = C'$.

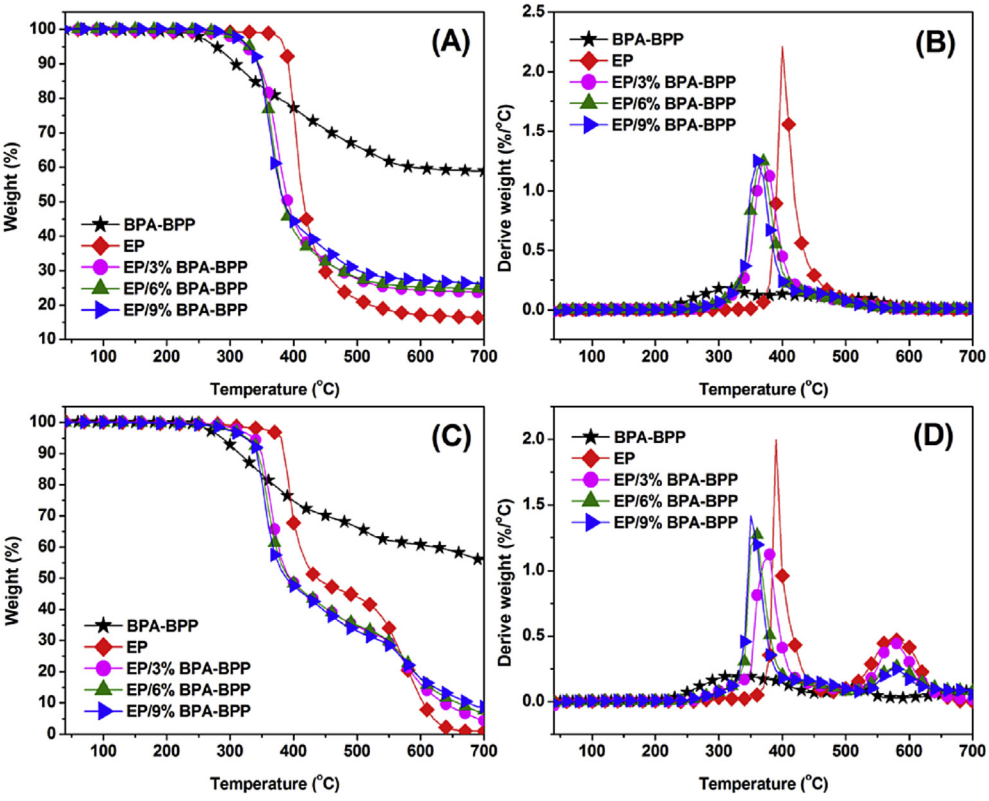

Fig. 5. TG (A, C) and DTG (B, D) curves of the synthesized BPA-BPP, neat EP, and EP/BPA-BPP composites under a nitrogen (A, B) or an air (C, D) atmosphere.

Table 3
Typical parameters from TG analyses under nitrogen and air atmosphere.[a]

	Samples	T_{onset} (°C)	T_{max1} (°C)	T_{max2} (°C)	α_{max1} (%/°C)	α_{max2} (%/°C)	Residue at 500 °C (wt%)	Residue at 700 °C (wt%)	
								Test values	Calculated values
N_2	BPA-BPP	276.2	305.9	/	0.189	/	66.1	58.9	/
	EP	386.1	400.8	/	2.230	/	21.7	16.4	/
	EP/3%BPA-BPP	331.7	371.3	/	1.296	/	27.6	23.7	17.7
	EP/6%BPA-BPP	330.5	365.9	/	1.301	/	28.0	24.7	19.0
	EP/9%BPA-BPP	328.9	360.3	/	1.250	/	30.1	26.3	20.2
Air	BPA-BPP	284.7	345.3	393.7	0.201	0.161	66.4	56.1	/
	EP	380.7	390.6	573.8	2.010	0.476	44.0	0.8	/
	EP/3%BPA-BPP	337.0	359.1	577.6	1.271	0.297	34.6	4.4	2.5
	EP/6%BPA-BPP	326.2	355.8	577.3	1.340	0.264	34.9	7.6	4.1
	EP/9%BPA-BPP	324.1	354.0	576.4	1.498	0.248	33.0	8.7	5.8

[a] T_{onset}: Initial decomposition temperature (based on 5% weight loss); T_{max}: Maximum weight-loss temperature; α_{max}: Maximum weight loss rate.

Table 4
LOI and UL-94 results of the EPs.

Sample	LOI (vol%)	UL-94 (3.2 mm)				P content[b] (wt%)
		t_1(s)[a]	t_2(s)[a]	Rating	Dripping	
EP	21.0	>50	–	NR	Yes	0
EP/3%BPA-BPP	26.8	>50	–	NR	No	0.414
EP/6%BPA-BPP	28.2	32.7	2.1	NR	No	0.828
EP/9%BPA-BPP	28.7	28.2	0	V-1	No	1.242

[a] Average combustion duration after the first (t_1) and the second ignition (t_2).
[b] P content are calculated according to the P-contents in BPA-BPP (13.8 wt% reported by ICP-OES test) and additive amounts of BPA-BPP in EP.

BPP sample is burnt more than 50 s. Obviously, the incorporation of BPA-BPP (3 wt%~9 wt%) can improve the flame retardancy of epoxy resins. Unfortunately, the flame retadancy of EP thermosets is not enhanced when the loadings of BPA-BPP are increased. The formulas and flame retardancy results of EPs with 12 wt% and 15 wt% BPA-BPP are summarized in Table S2 (Supporting information) The results show that the flame-retardant sample with higher content of BPA-BPP (12 wt% and 15 wt%) can also only pass V-1 rating, whereas the LOI values of which are decreased. These results can be attributed to that EP with more BPA-BPP could produce excessive gases products (aniline etc.), affecting the compactness of char-layers during combustion. Meanwhile, aniline is a type of flammable product. These samples are difficult to extinguish in LOI and UL-94 tests. Based on this, we did not investigate the performances of the EP samples with 12 wt% and 15 wt% BPA-BPP any longer in other tests.

The microscale combustion calorimeter (MCC) based on oxygen consumption calorimetry is well known as pyrolysis combustion flow calorimetry (PCFC) [29–31]. From just a few milligrams of samples, MCC can quickly and easily provide the key flammability parameters of the materials, such as peak heat release rate (pHRR), total heat released (THR), and temperature at pHRR (T_p). The heat release rate (HRR) curves of neat EP and EP with different contents of BPA-BPP composites are shown in Fig. 7, and the corresponding data are presented in Table 5. It can be observed that the addition of BPA-BPP reduces the pHRR and THR values compared to neat EP sample obviously. When 3 wt%, 6 wt% and 9 wt% BPA-BPP has been separately incorporated, the pHRR values of flame retardant EP samples are lowered to 482.8, 450.1 and 433.8 W/g from 709.6 W/g of neat EP, respectively. The THR values of the EP/BPA-BPP composites are also decreased by 16.4%, 20.1% and 20.7% in comparison with neat EP. The T_p of EP/BPA-BPP composites decreased gradually with the increasement of BPA-BPP. It is because the incorporation of BPA-BPP promotes earlier decomposition of EP and forms protective chars. These results are essentially in agreement with the TGA analyses mentioned above.

Although MCC has many benefits to evaluate the flame-retadancy of polymers, this method fails to account for physical effects, such as dripping or intumescence [32]. The cone calorimeter, which is an effective test similar to the real fire based on oxygen consumption principle [33–35], has been used to evaluate the fire performance of neat EP and EP/9%BPA-BPP. The typical curves and corresponding data are shown in Fig. 8 and Table 6. The peak of the heat release rate (PHRR) and the total heat release (THR) of EP/9%BPA-BPP are only 457 kW/m^2 and 78.4 MJ/m^2, which are declined by 60.1% and 11.3% compared with neat EP (1148 kW/m^2, 88.4 MJ/m^2), respectively. Two important parameters, fire growth rate (FIGRA) and maximum average rate of heat emission (MAHRE) have been used to estimate the fire safety of EPs. FIGRA is defined as the value dividing the PHRR by the time to PHRR (t_p) [36,37]. According to the definition, lower FIGRA values suggest that the time to flashover is delayed, which provide enough escape time for people in conflagration [38]. Then, compared to neat EP, a better fire safety of EP/9%BPA-BPP is obtained owing to the decreases of both FIGRA (8.5–3.0 kW/m^2/s) and MAHRE (312.0–207.0 kW/m^2) as shown in Table 6. The lower FIGRA value and MAHRE value should be attributed to the longer t_p of EP/9%BPA-BPP and the decreases PHRR and THR values, respectively. Notably, the decreases of total smoke production (TSP) and total smoke release (TSR) values of EP/9%BPA-BPP suggest that BPA-BPP could improve the smoke inhibition of EP (Fig. 8 (D) and Table 6). Furthermore, char residue of EP/BPA-BPP are enhanced from 4.4 wt% to 22.7 wt%. The time to ignition (TTI) of EP with 9 wt% BPA-BPP is shorter, which can be explained to the earlier decomposition of EP/9%BPA-BPP than that of EP, according to the results from TGA.

3.4. Char residue analysis

The char residues play a significant role in improving flame retardancy of epoxy resins; the investigation of combustion residues is favorite of achieving great understanding of mechanism of BPA-BPP. Both the exterior and the interior char layers from the LOI tests have been analyzed via SEM. The samples for both EP and flame-retardant EP were collected after LOI tests at their highest testing concentration of oxygen, respectively. The photographs of neat EP and EP/9%BPA-BPP after LOI test and their corresponding morphologies are illustrated in Fig. 9. A soft and broken char layer of neat EP is left after burning (Fig. 9 A). Meanwhile, outer and inner surface micromor-phologies of this char are thin and fragile (Fig. 9 a1 and a2). Thus, neat EP is inflammability and hardly self-extinguished in LOI test. When 9 wt% BPA-BPP is incorporated into epoxy resins, char layers with the compact outer surface and honeycombed inner surface could be observed in Fig. 9 (b1) and (b2). It obviously displayed that a little intumenscent (vertical direction in particular) and completed char layers of EP/9%BPA-BPP

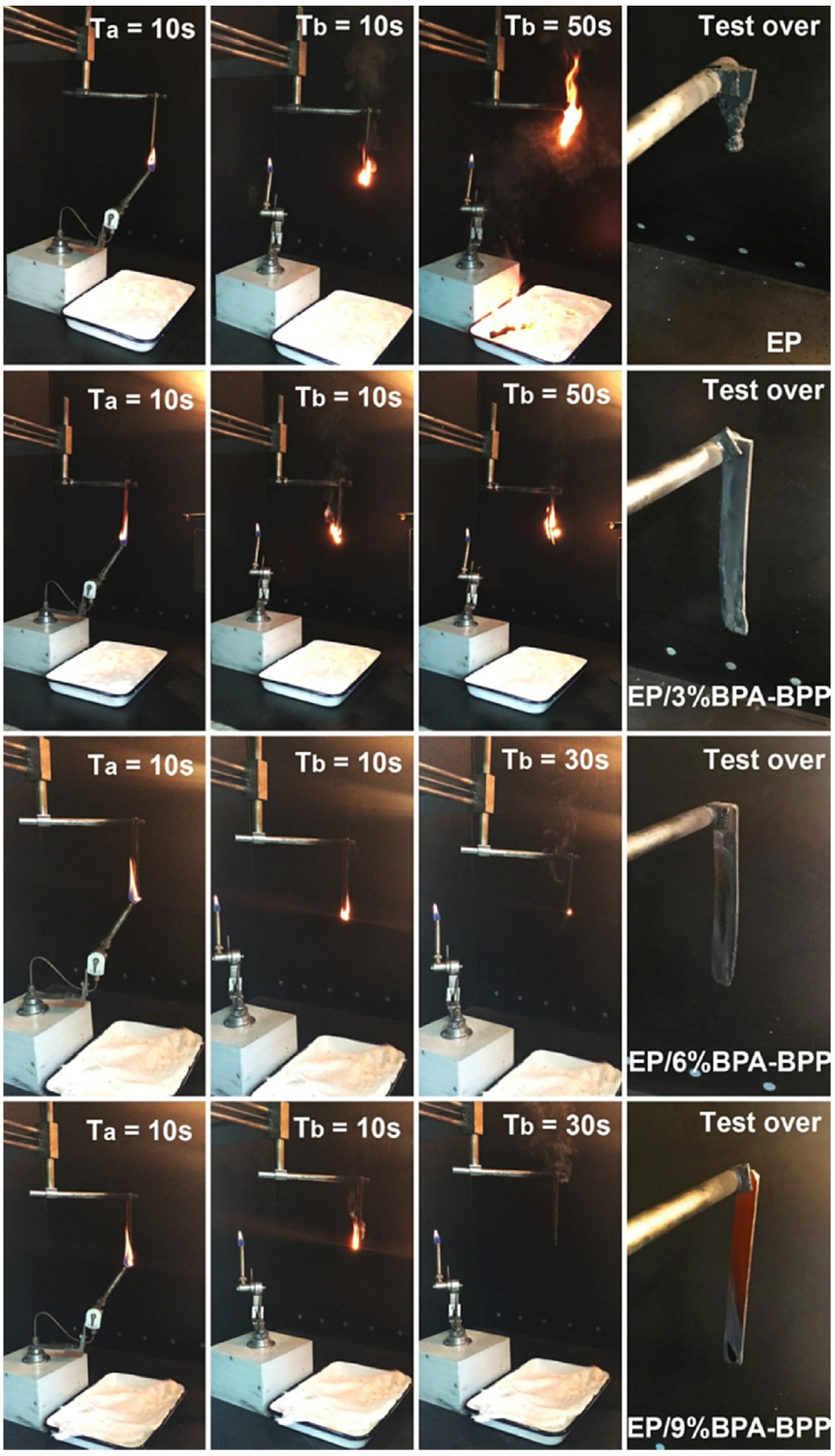

Fig. 6. Photographs of the EPs recorded during UL-94 tests. T_a, the first 10 s ignition; T_b, the time after the first ignition.

have been formed after LOI test (Fig. 9 B). It is speculated that the intumenscent char layers with honeycombed inner surface is attributed to the release of plenty of gases during heating, which is confirmed in following pyrolysis test. The improving flame retardancy of EP/BPA-BPP samples mainly depends on this intumenscent char, which acts as insulating barrier to prevent the oxygen and the feedback of heat from reaching the underling material during the process of combustion.

Laser Raman spectroscopy has been recognized to be an effective analysis technique to investigate carbonaceous char layers of the polymers produced during burning [39–41]. In this work, Raman spectroscopy was employed to study the residue chars of neat EP and EP/BPA-BPP composites from LOI tests. As shown in Fig. 10, the D-band at about 1355 cm^{-1} and the G-band at around 1587 cm^{-1} are attributed to the vibrations of the amorphous char, and the vibration of sp^2-hybridized carbon atoms in a graphite

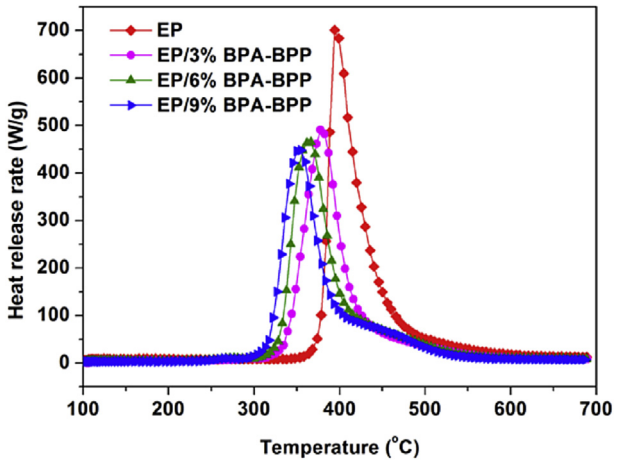

Fig. 7. Heat release rate curves of cured epoxy resins from MCC tests.

Table 5
Combustion parameters of the EP composites obtained from MCC test.

Sample	pHRR (W/g)	THR (kJ/g)	T_p (°C)
EP	709.6	32.8	395.9
EP/3%BPA-BPP	482.8	27.4	379.6
EP/6%BPA-BPP	450.1	26.2	363.8
EP/9%BPA-BPP	433.8	26.0	352.8

shield efficiency [44].

The chemical compositions of residue chars are further analyzed by FTIR spectroscopy. Fig. 11 depicts the FTIR spectra of the residue chars of neat EP and EP/9%BPA-BPP. A series of absorption peaks at 1593, 1503, and 1455 cm^{-1} can be attributed to aromatics and polyaromatics formed during combustion. Compared to the char of neat EP, the peak at 1082 cm^{-1} corresponding to the stretching vibration of P—*O*—P bond, indicates the formation of polyphosphoric acids. The absorption peaks of P—*O*—C bond at 1015 and 894 cm^{-1} suggest that the residue chars contain phosphorus oxides together with carbon ones. The peaks of N—P═N at 1180 and 1145 cm^{-1} indicate that the residue chars remain phosphazenes derivatives. A weak characteristic band at 3035-2865 cm^{-1} is due to the organic part of the char. These results indicate that the residual chars mainly consist of phosphor-carbonaceous and phosphor-oxidative solids as well as highly carbonized aromatic networks.

3.5. The Py-GC/MS of BPA-BPP

To further elucidate the pyrolysis behavior as well as the flame-retardant mechanism, BPA-BPP was rapidly pyrolyzed at 500 °C wherein the pyrolysis products were separated and detected via GC/MS. The pyrolysis temperature is chosen at 500 °C because it is close to the ignition temperature of epoxy resin according to the Py-GC/MS measuring parameters in some relevant articles [24,45]. The gas-chromatogram and corresponding mass-spectrograms of pyrolysis products during pyrolysis are shown in Fig. 12 and Fig. 13,

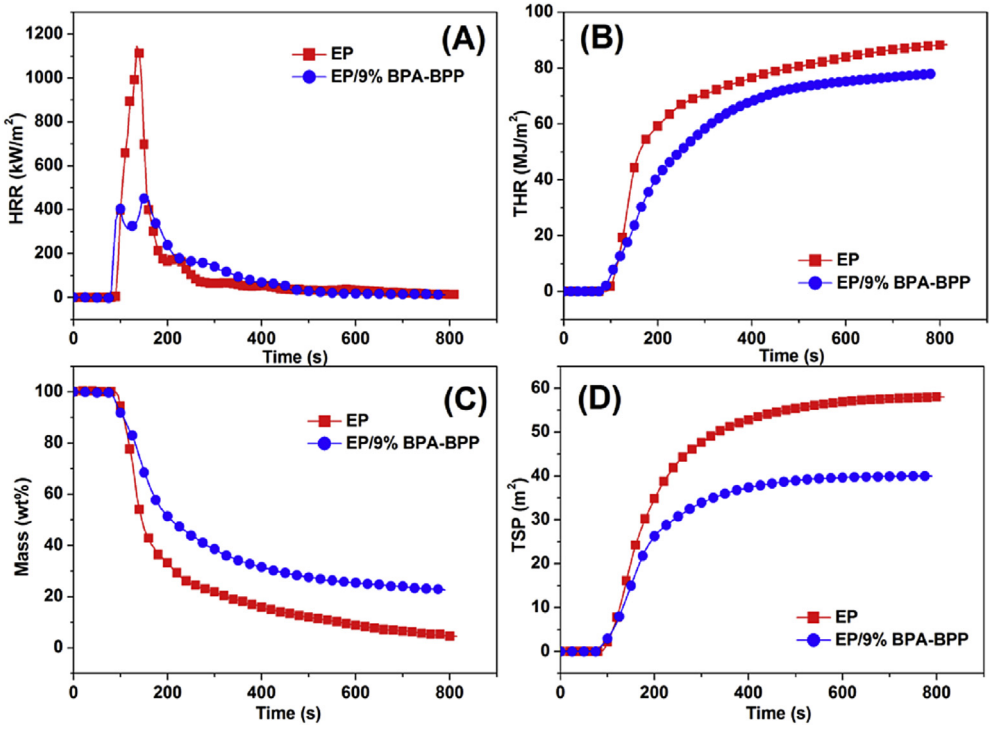

Fig. 8. Curves of EP and EP/9%BPA-BPP from cone calorimeter tests. (A) HRR, (B) THR, (C) residue mass and (D) TSP.

layer, respectively [42]. The intensity ratio I_D/I_G (noted as R) is conversely proportional to the in-plane micro-crystalline size [43]. The calculated results indicate that the residue char of EP/9%BPA-BPP exhibits a greater R value (2.04) than that of neat EP (1.29). The larger R value of EP/9%BPA-BPP indicates a smaller size of carbonaceous microstructures, which is related to higher protective

respectively. The three main peaks which denote three pyrolysis products appear at 2.36–2.79, 8.95 and 17.88 min (Fig. 12). Fig. 13 further confirms that these pyrolysis products are 2,3-Dimethylbutane ($[M-1]^+ = 85$), aniline ($M^+ = 93$) and diphenylamine ($M^+ = 169$). It is deduced that these volatile fragments mainly arose from decomposition of substituents attached to the

Table 6
Cone calorimeter data of EP and EP/9%BPA-BPP.

Samples	TTI (s)	PHRR (kW/m^2)	THR (MJ/m^2)	t_p[a] (s)	FIGRA[b] (kW/m^2/s)	MAHRE[c] (kW/m^2)	TSR (m^2/m^2)	TSP (m^2)	Residue (wt%)
EP	82	1148	88.4	135	8.5	312.0	6564	58	4.4
EP/9%BPA-BPP	72	457	78.4	150	3.0	207.0	4522	40	22.7

[a] t_p means time to PHRR.
[b] FIGRA is calculated by dividing the PHRR by t_p.
[c] AHRE means average rate of heat emission, which is defined as the cumulative heat emission divided by time; MAHRE denotes the maximum average rate of heat emission.

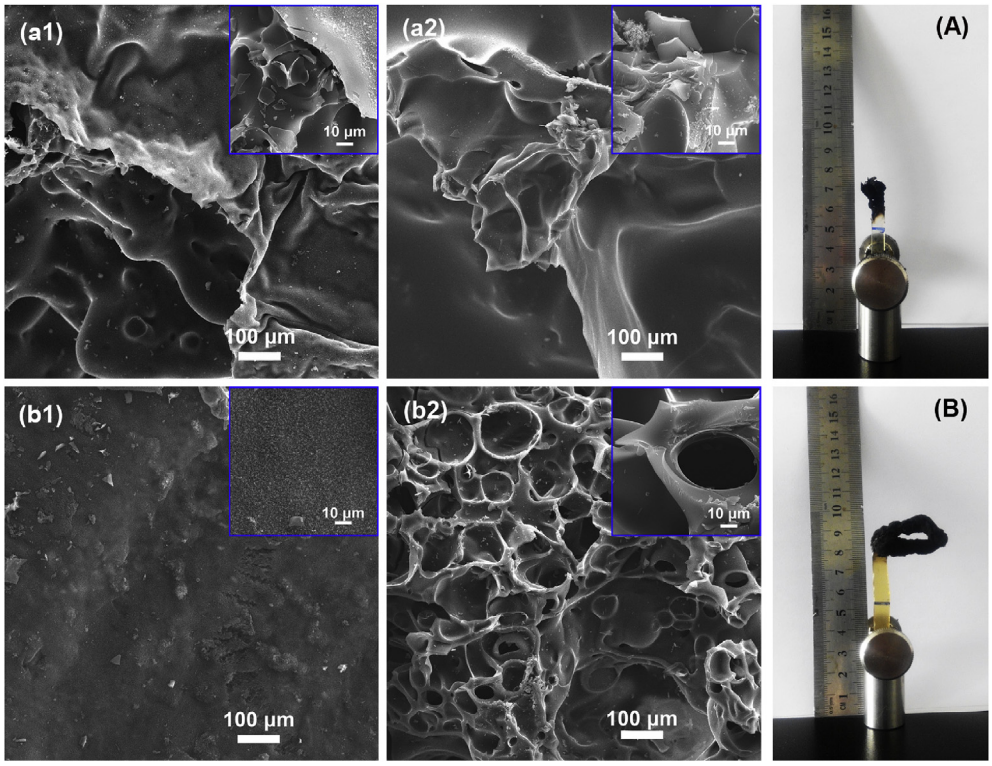

Fig. 9. Scanning electron micrographs (× 100, × 1000) of EP/BPA-BPP composites char after LOI tests: the outer and inner surface of neat EP (a1, a2) and EP/9%BPA-BPP(b1, b2); Photographs of the specimens after LOI test: the neat EP (A) and EP/9%BPA-BPP (B).

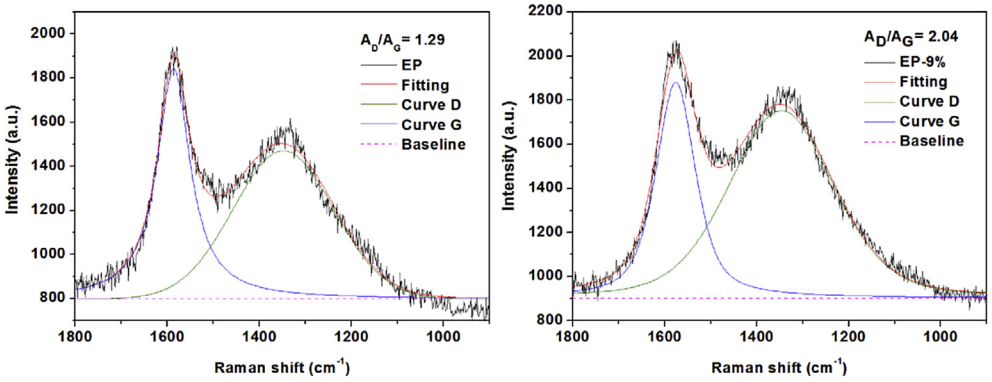

Fig. 10. Raman spectra of residue chars of EP and EP/9%BPA-BPP.

phosphazene ring. Notably, the pyrolysis products containing phosphorous cannot be detected in gaseous phase which suggests that the cyclotriphosphazenes have still been remained in the residue according to the work of Zhang and his co-workers [46]. In order to prove this viewpoint, the residue char of BPA-BPP obtained at 500 °C for 10 min under N_2 were characterized by FTIR. It is obvious that the absorption peak of N–P=N are located at 1160 cm^{-1} (Fig. S1 in supporting information). Moreover, the P and N contents in both BPA-BPP and in the residue of BPA-BPP after heating at 500 °C (N_2) were also tested. These corresponding data

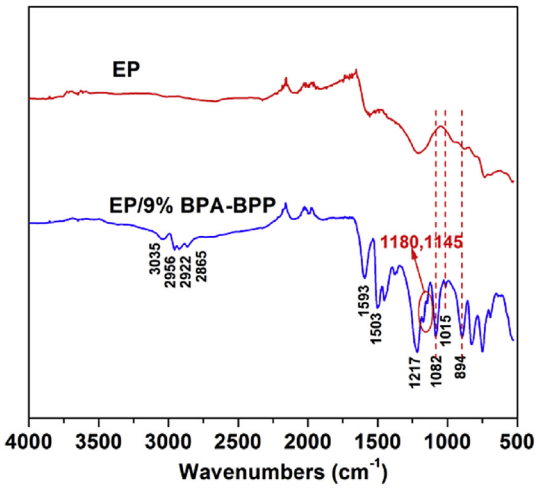

Fig. 11. FTIR spectra of the residue char after LOI tests.

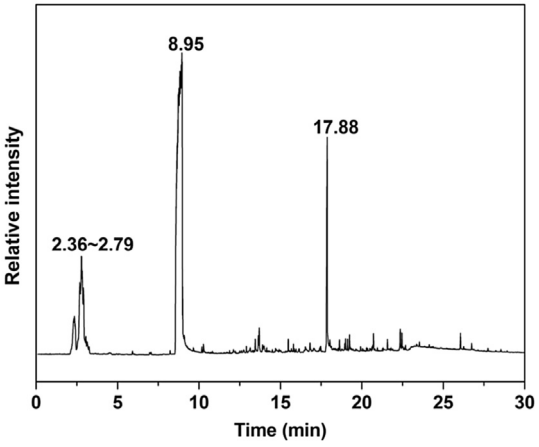

Fig. 12. The gas-chromatogram of the pyrolysis products.

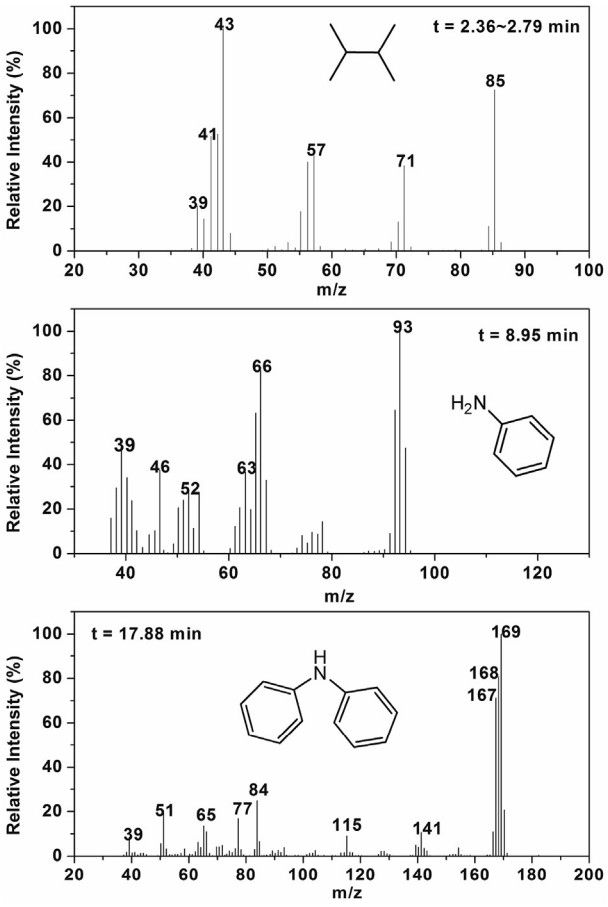

Fig. 13. Typical mass-spectrograms of BPA-BPP at different retention time according to gas-chromatogram.

are listed in Table S3, wherein both the P and N contents of the residue char of BPA-BPP are higher than those of BPA-BPP, indicating that plenty of P and N are left in the residue. In addition, the ratio of P/N of the char residue is 1.01 (21.9/21.7) which is close to the P/N ratio of cyclotriphosphazenes (1.29). The slightly higher value of N amount could be explained to the incomplete decomposition of BPA-BPP at 500 °C. Based on these analyses, we believe that the cyclotriphosphazenes have still been remained in the residue.

Scheme 2 illustrates the possible degradation pathway for BPA-BPP according to pyrolysis results, which initiates the hemolytic cleavage of C–C bonds from the two phenyl groups and the isopropyliden group. The formed $N_3P_3(OPh)(NHPh)_5$ undergoes side-group condensation/elimination reactions, which are similar to the pyrolysis behaviors of the hexamethylaminocyclotriphosphazene $[NP(NHCH_3)_2]_3$ and anilinocyclophosphazenes $[NP(NHPh)_2]_3$ [47–50]. Aniline and diphenylamine are formed in gaseous phase via relative free radical reaction. In addition, NH_3 could be also released in gaseous phase from the continuous decomposition of aniline and diphenylamine, although the detection for NH_3 (17 g/mol) cannot be observed in Py-GC/MS test with scanning parameter of mass spectrometric starting from $m/z = 35$. These products released in gaseous phase could act as a foaming agent and cause intumencent char layers which are in agreement with the photo of EP/9%BPA-BPP (Fig. 9 B). Combining the char residue and thermogravimetric analyses above, BPA-BPP might eventually leave a cross-linked material which closely approximate to the composition of the heterogeneous graphitic/phosphorus nitride residue in condensed phase according to the similar report [50].

According to the investigation of volatile decomposition products, char morphology and architecture, it can be deduced that BPA-BPP in the system can act as a catalyst for char formation and a foaming agent. When the EP/BPA-BPP composites are exposed to fire or heat, BPA-BPP begins to decompose and releases aniline, diphenylamine and NH_3. Intumencent and continuous char layers are formed with release and flow of these gases. Meanwhile, phosphorus-rich carbonaceous char in condensed phase can act as a barrier to prevent the diffusion of gaseous products to the flame and shield the polymer surface from heat and air during combustion [51].

4. Conclusions

A novel bridged-cyclotriphosphazene flame retardant BPA-BPP was successfully synthesized by nucleophilic substitution reaction of hexachlorocyclotriphosphazene, bisphenol-A and aniline. BPA-BPP was then mixed with DGEBA and DDM to fabricate the flame retardant epoxy resins. The study on thermal properties showed that the initial decomposition temperatures of EP/BPA-BPP were lower than those of neat EP, whereas their thermal stability and char yields improved significantly at high temperature. It was

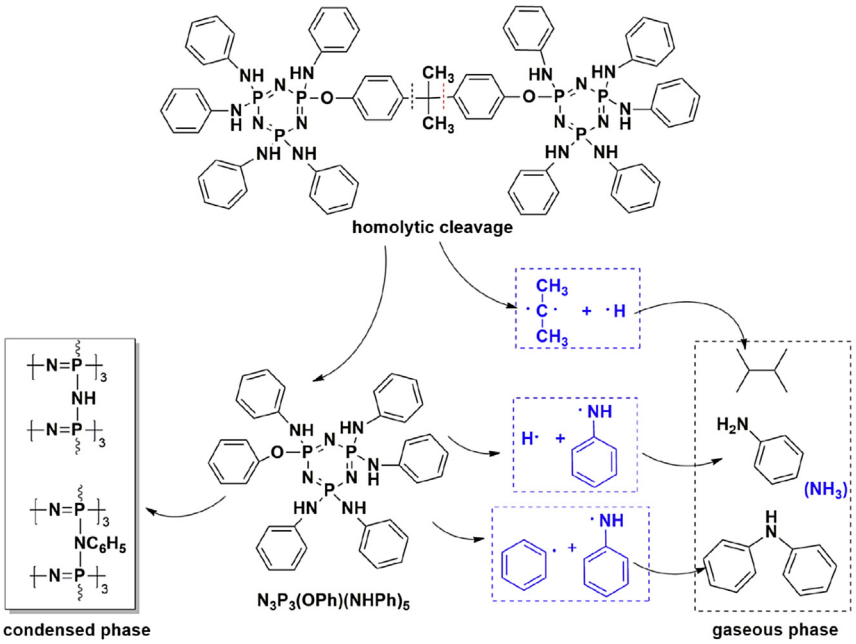

Scheme 2. The possible pyrolysis route of BPA-BPP.

confirmed that EP/BPA-BPP exhibited excellent flame retardancy via LOI, UL-94 and MCC tests. From cone calorimetric test, PHRR and THR values of EP/9%BPA-BPP were greatly decreased; better fire safety and smoke suppression were also obtained. The char residue analysis via SEM, Raman and FTIR indicated that intumescent and completed char layers mainly consist of phosphor-carbonaceous and phosphor-oxidative solids as well as highly carbonized aromatic networks. This protective char layer could shield the underlying polymeric substrate from further burning. The Py-GC/MS results showed that aniline and diphenylamine were released in gaseous phase and the cyclotriphosphazenes still remained in condensed phase during the pyrolysis of BPA-BPP.

Acknowledgement

Financial support by the National Natural Science Foundation of China (Grant 51403191 and 51403040) are sincerely acknowledged.

Appendix A. Supplementary data

Supplementary data related to this article can be found at http://dx.doi.org/10.1016/j.polymdegradstab.2016.08.013.

References

[1] A. Zotti, A. Borriello, M. Ricciardi, V. Antonucci, M. Giordano, M. Zarrelli, Effects of sepiolite clay on degradation and fire behaviour of a bisphenol A-based epoxy, Compos. Part B. Eng. 73 (2015) 139–148.
[2] K. Zhou, J. Liu, Y. Shi, S. Jiang, D. Wang, Y. Hu, Z. Gui, MoS_2 nanolayers grown on carbon nanotubes: an advanced reinforcement for epoxy composites, ACS Appl. Mater. Inter 11 (2015) 6070–6081.
[3] T. Mariappan, C.A. Wilkie, Flame retardant epoxy resin for electrical and electronic applications, Fire Mater 5 (2014) 588–598.
[4] E.D. Weil, S. Levchik, A review of current flame retardant systems for epoxy resins, J. Fire Sci. 1 (2004) 25–40.
[5] B.W. Liu, H.B. Zhao, Y. Tan, L. Chen, Y.Z. Wang, Novel crosslinkable epoxy resins containing phenylacetylene and azobenzene groups: from thermal crosslinking to flame retardance, Polym. Degrad. Stab. 122 (2015) 66–76.
[6] J. Sun, Z.Y. Yu, X.D. Wang, D.Z. Wu, Synthesis and performance of cyclomatrix polyphosphazene derived from trispiro-cyclotriphosphazene as a halogen-free nonflammable material, ACS Sustain. Chem. Eng. 2 (2013) 231–238.
[7] N.M. Neisius, M. Lutz, D. Rentsch, P. Hemberger, S. Gaan, Synthesis of DOPO-based phosphonamidates and their thermal properties, Ind. Eng. Chem. Res. 8 (2014) 2889–2896.
[8] G. You, Z. Cheng, H. Peng, H. He, The synthesis and characterization of a novel phosphorus-nitrogen containing flame retardant and its application in epoxy resins, J. Appl. Polym. Sci. 22 (2014) 41079.
[9] J.Y. Wang, L.J. Qian, B. Xu, W. Xi, X.X. Liu, Synthesis and characterization of aluminum poly-hexamethylenephosphinate and its flame-retardant application in epoxy resin, Polym. Degrad. Stab. 122 (2015) 8–17.
[10] M.J. Xu, G.R. Xu, Y. Leng, B. Li, Synthesis of a novel flame retardant based on cyclotriphosphazene and DOPO groups and its application in epoxy resins, Polym. Degrad. Stab. 123 (2016) 105–114.
[11] J. Sun, X.D. Wang, D.Z. Wu, Novel spirocyclic phosphazene-based epoxy resin for halogen-free fire resistance: synthesis, curing behaviors, and flammability characteristics, ACS Appl. Mater. Inter 8 (2012) 4047–4061.
[12] Y. Tan, Z.B. Shao, X.F. Chen, J.W. Long, L. Chen, Y.Z. Wang, Novel multifunctional organic–inorganic hybrid curing agent with high flame-retardant efficiency for epoxy resin, ACS Appl. Mater. Inter 32 (2015) 17919–17928.
[13] C. Xie, B. Zeng, H. Gao, Y. Xu, W. Luo, X. Liu, L. Dai, Improving thermal and flame-retardant properties of epoxy resins by a novel reactive phosphorous-containing curing agent, Polym. Eng. Sci. 5 (2014) 1192–1200.
[14] L.J. Qian, L.J. Ye, Y. Qiu, S.R. Qu, Thermal degradation behavior of the compound containing phosphaphenanthrene and phosphazene groups and its flame retardant mechanism on epoxy resin, Polymer 24 (2011) 5486–5493.
[15] G.R. Xu, M.J. Xu, B. Li, Synthesis and characterization of a novel epoxy resin based on cyclotriphosphazene and its thermal degradation and flammability performance, Polym. Degrad. Stab. 109 (2014) 240–248.
[16] K.R. Fontenot, M.M. Nguyen, M.S. Al-Abdul-Wahid, M.W. Easson, S. Chang, G.A. Lorigan, B.D. Condon, The thermal degradation pathway studies of a phosphazene derivative on cotton fabric, Polym. Degrad. Stab. 120 (2015) 32–41.
[17] Z.P. Mao, J.W. Li, F. Pan, X.D. Zeng, L.P. Zhang, Y. Zhong, X. Sui, H. Xu, High-temperature auto-cross-linking cyclotriphosphaznene: synthesis and application in flame retardance and antidripping poly (ethylene terephthalate), Ind. Eng. Chem. Res. 15 (2015) 3788–3799.
[18] R. Yang, W. Hu, L. Xu, Y. Song, J.C. Chun, Synthesis, mechanical properties and fire behaviors of rigid polyurethane foam with a reactive flame retardant containing phosphazene and phosphate, Polym. Degrad. Stab. 122 (2015) 102–109.
[19] H.R. Allcock, New approaches to hybrid polymers that contain phosphazene rings, J. Inorg. Organomet. Polym. 2 (2007) 349–359.
[20] M. El Gouri, A. El Bachiri, S.E. Hegazi, M. Rafik, A. El Harfi, Thermal degradation of a reactive flame retardant based on cyclotriphosphazene and its blend with DGEBA epoxy resin, Polym. Degrad. Stab. 11 (2009) 2101–2106.
[21] H. Liu, X. Wang, D. Wu, Novel cyclotriphosphazene-based epoxy compound and its application in halogen-free epoxy thermosetting systems: synthesis, curing behaviors, and flame retardancy, Polym. Degrad. Stab. 103 (2014) 96–112.
[22] H.R. Allcock, Recent developments in polyphosphazene materials science, Curr. Opin. Solid State Mater. Sci. 5 (2006) 231–240.
[23] P. Jiang, X. Gu, S. Zhang, J. Sun, R. Xu, S. Bourbigot, S. Duquesne, M. Casetta,

Flammability and thermal degradation of poly (lactic acid)/polycarbonate alloys containing a phosphazene derivative and trisilanollsobutyl POSS, Polymer 79 (2015) 221–231.
[24] S. Yang, J. Wang, S. Huo, J. Wang, Y. Tang, Synthesis of a phosphorus/nitrogen-containing compound based on maleimide and cyclotriphosphazene and its flame-retardant mechanism on epoxy resin, Polym. Degrad. Stab. 126 (2016) 9–16.
[25] M. El Gouri, S.E. Hegazi, M. Rafik, A. El Harfi, Synthesis and thermal degradation of phosphazene containing the epoxy group, Ann. Chim. Sci. Mat. 1 (2010) 27–39.
[26] C. Liu, T. Chen, C. Yuan, C. Song, Y. Chang, G. Chen, Y. Xu, L. Dai, Modification of epoxy resin through the self-assembly of a surfactant-like multi-element flame retardant, J. Mater. Chem. A 4 (2016) 3462–3470.
[27] X. Zhang, Q. He, H. Gu, H.A. Colorado, S. Wei, Z. Guo, Flame-retardant electrical conductive nanopolymers based on bisphenol F epoxy resin reinforced with nano polyanilines, ACS Appl. Mater. Inter 5 (2013) 898–910.
[28] K. Wu, L. Song, Y. Hu, H. Lu, B.K. Kandola, E. Kandare, Synthesis and characterization of a functional polyhedral oligomeric silsesquioxane and its flame retardancy in epoxy resin, Prog. Org. Coat. 65 (2009) 490–497.
[29] R.E. Lyon, R. Walters, S. Stoliarov, Screening flame retardants for plastics using microscale combustion calorimetry, Polym. Eng. Sci. 47 (2007) 1501–1510.
[30] X. Wang, Y. Hu, L. Song, W. Xing, H. Lu, Preparation, flame retardancy, and thermal degradation of epoxy thermosets modified with phosphorous/nitrogen-containing glycidyl derivative, Polym. Adv. Technol. 23 (2012) 190–197.
[31] C.Q. Yang, Q. He, R.E. Lyon, Y. Hu, Investigation of the flammability of different textile fabrics using micro-scale combustion calorimetry, Polym. Degrad. Stab. 95 (2010) 108–115.
[32] B. Schartel, K.H. Pawlowski, R.E. Lyon, Pyrolysis combustion flow calorimeter: a tool to assess flame retarded PC/ABS materials? Thermochim. Acta 462 (2007) 1–14.
[33] B. Schartel, T.R. Hull, Development of fire-retarded materials-interpretation of cone calorimeter data, Fire Mater 31 (2007) 327–354.
[34] A.B. Morgan, M. Bundy, Cone calorimeter analysis of UL-94 V-rated plastics, Fire Mater 31 (2007) 257–283.
[35] C.A. Wilkie, G. Chigwada, J.W.G. Sr, R.E. Lyon, High-throughput techniques for the evaluation of fire retardancy, J. Mater. Chem. 16 (2006) 2023–2030.
[36] M. Sacristán, T.R. Hull, A.A. Stec, J.C. Ronda, M. Galià, V. Cádiz, Cone calorimetry studies of fire retardant soybean-oil-based copolymers containing silicon or boron: comparison of additive and reactive approaches, Polym. Degrad. Stab. 95 (2010) 1269–1274.
[37] B. Zhao, L. Chen, J.W. Long, H.B. Chen, Y.Z. Wang, Aluminum hypophosphite versus alkyl-substituted phosphinate in polyamide 6: flame retardance, thermal degradation, and pyrolysis behavior, Ind. Eng. Chem. Res. 52 (2013) 2875–2886.
[38] C. Katsoulis, E. Kandare, B.K. Kandola, in: T.R. Hull, B.K. Kandola (Eds.), Thermal and Fire Performance of Flame-retarded Epoxy Resin: Investigating Interaction between Resorcinol Bis (Diphenyl Phosphate) and Epoxy Nanocomposites, Royal Society of Chemistry, Cambridge, U.K, 2009. Chapter 17, 184–205.
[39] R. Xie, B. Qu, Expandable graphite systems for halogen-free flame-retarding of polyolefins. I. Flammability characterization and synergistic effect, J. Appl. Polym. Sci. 80 (2001) 1181–1189.
[40] L. Li, P. Wei, J. Li, J. Jow, K. Su, Synthesis and characterization of a novel flame retardant and its application in polycarbonate, J. Fire Sci. 28 (2010) 523–538.
[41] B. Zhao, L. Chen, J.W. Long, R.K. Jian, Y.Z. Wang, Synergistic effect between aluminum hypophosphite and alkyl-substituted phosphinate in flame-retarded polyamide 6, Ind. Eng. Chem. Res. 52 (2013) 17162–17170.
[42] H.B. Zhao, B.W. Liu, X.L. Wang, L. Chen, X.L. Wang, Y.Z. Wang, A flame-retardant-free and thermo-cross-linkable copolyester: flame-retardant and anti-dripping mode of action, Polymer 55 (2014) 2394–2403.
[43] F. Tuinstra, J.L. Koenig, Raman spectrum of graphite, J. Chem. Phys. 53 (1970) 1126–1130.
[44] S. Bourbigot, M. Le Bras, R. Delobel, R. Decressain, J.P. Amoureux, Synergistic effect of zeolite in an intumescence process: study of the carbonaceous structures using solid-state NMR, J. Chem. Soc. Faraday Trans. 92 (1996) 149–158.
[45] L.J. Qian, L. J Ye, Y. Qiu, S.R. Qu, Thermal degradation behavior of the compound containing phosphaphenanthrene and phosphazene groups and its flame retardant mechanism on epoxy resin, Polymer 52 (2011) 5486–5493.
[46] X. Zhang, Y. Zhong, Z.P. Mao, The flame retardancy and thermal stability properties of poly (ethylene terephthalate)/hexakis (4-nitrophenoxy) cyclotriphosphazene systems, Polym. Degrad. Stab. 97 (2012) 1504–1510.
[47] H. Allcock, C. Kolich, W. Kossa, Pyrolysis of aminophosphazenes, Inorg. Chem. 16 (1977) 3362–3364.
[48] H. Allcock, D. Patterson, Phosphorus-nitrogen compounds. 27. Ring-ring and ring-chain equilibration of dimethylphosphazenes, Relation to phosphazene polymerization, Inorg. Chem. 16 (1977) 197–200.
[49] A. Ballistreri, S. Foti, G. Montaudo, S. Lora, G. Pezzin, Mass spectrometric characterization and thermal decomposition mechanism of some poly (organophosphazenes), Makromo, Chem. Rapid Commun. 182 (1981) 1319–1326.
[50] H.R. Allcock, G.S. McDonnell, G.H. Riding, I. Manners, Influence of different organic side groups on the thermal behavior of polyphosphazenes: random chain cleavage, depolymerization, and pyrolytic cross-linking, Chem. Mater 2 (1990) 425–432.
[51] S.Y. Lu, I. Hamerton, Recent developments in the chemistry of halogen-free flame retardant polymers, Prog. Polym. Sci. 27 (2002) 1661–1712.